ACI STRUCTURAL JOURNAL TECHNICAL PAPER

Title no. 104-S70

Textile-Reinforced Mortar versus Fiber-Reinforced Polymer Confinement in Reinforced Concrete Columns

by Dionysios A. Bournas, Panagiota V. Lontou, Catherine G. Papanicolaou, and Thanasis C. Triantafillou

The effectiveness of textile-reinforced mortar (TRM) jackets as a means of confining reinforced concrete (RC) columns with limited capacity due to buckling of the longitudinal bars is experimentally investigated in this study. Comparisons with fiber-reinforced polymer (FRP) jackets of equal stiffness and strength allow for the evaluation of the effectiveness of TRM versus FRP. Tests were carried out both on short prisms under concentric compression and on nearly full-scale, nonseismically detailed, RC columns subjected to cyclic uniaxial flexure under constant axial load. The compression tests on 15 RC prisms show that TRM jackets provide a substantial gain in compressive strength and deformation capacity by delaying buckling of the longitudinal bars; this gain increases with the volumetric ratio of the jacket. Compared with their FRP counterparts, TRM jackets used in this study are slightly less effective in terms of increasing strength and deformation capacity by approximately 10%. Tests on nearly full-scale columns under cyclic uniaxial flexure show that TRM jacketing is very effective (and equally to its FRP counterpart) as a means of increasing the cyclic deformation capacity and the energy dissipation of old-type RC columns with poor detailing by delaying bar buckling. The test results presented in this study indicate that TRM jacketing is an extremely promising solution for the confinement of RC columns, including poorly detailed ones in seismic regions.

Keywords: bars; buckling; confinement; fiber-reinforced polymer; seismic retrofitting; textile-reinforced mortar.

INTRODUCTION AND BACKGROUND

The upgrading of existing reinforced concrete (RC) structures through jacketing of columns has become the method of choice in an increasingly large number of rehabilitation projects, mainly seismic but also nonseismic. Among all jacketing techniques, the use of fiber-reinforced polymers has substantially gained popularity in the structural engineering community due to the favorable properties offered by these materials (high strength-to-weight ratio, corrosion resistance, ease and speed of application, and minimal change of geometry). Despite all the advantages, the fiber-reinforced polymer (FRP) retrofitting technique has a few drawbacks (for example, poor behavior at high temperatures, high costs, inapplicability on wet surfaces, and difficulty to conduct post-earthquake assessment behind FRP jackets), which are mainly attributed to the organic (typically epoxy) resins used to bind the fibers. An interesting alternative to FRP materials are the so-called textile-reinforced mortars (TRMs).[1] These materials comprise textiles that are fabric meshes made of long woven, knitted, or even unwoven fiber rovings in at least two (typically orthogonal) directions, impregnated with inorganic binders such as cement-based mortars. The density—that is, the quantity and the spacing—of rovings in each direction can be controlled independently, thus affecting the mechanical characteristics of the textile and the degree of penetration of the mortar matrix through the mesh.

Although research on the use of textile meshes as reinforcement of cementitious products commenced in the early 1980s, developments in this field progressed rather slowly until the late 1990s. During the past few years, however, the research community has put considerable effort on the use of textiles as reinforcement of cement-based products (leading to the introduction of textile-reinforced concrete) primarily in new construction.[2-17] Studies on the use of textiles in the upgrading of concrete structures have been limited. Most of these studies have focused on flexural or shear strengthening of beams and on aspects of bond between concrete and cement-based textile composites[18-22]; these studies concluded that properly designed textiles combined with inorganic binders have a good potential as strengthening materials of RC members. The first study reported in the international literature on the use of textiles in combination with cement-based binders for the confinement of concrete is described in References 1 and 23. In this study, the authors experimentally investigated the application of TRM as a means of increasing the axial capacity of plain concrete through confinement. They also compared the behavior of TRM-confined cylinders and prisms with that of specimens confined with FRP jackets of equal stiffness and strength. The main conclusions were that: a) TRM jacketing provides a substantial gain in compressive strength and deformation capacity of plain concrete; and b) compared with their FRP counterparts, TRM jackets may result in slightly reduced effectiveness.

This study goes one step further by experimentally investigating the use of TRM jackets as a means of confining poorly detailed RC columns, which suffer from limited deformation capacity under seismic loads due to buckling of the longitudinal bars. Tests were carried out both on short prisms under concentric compression, reproducing the behavior of compression zones in RC members where bar buckling is critical, and on nearly full-scale nonseismically detailed RC columns subjected to cyclic uniaxial flexure under constant axial load. All specimens retrofitted with TRM jackets had their FRP-retrofitted counterpart, which enabled comparisons of the two systems.

RESEARCH SIGNIFICANCE

Jacketing of RC columns in existing structures is an increasingly attractive retrofit option. Among all jacketing techniques, the use of FRP has gained increasing popularity due to the favorable properties possessed by these materials.

ACI Structural Journal, V. 104, No. 6, November-December 2007.
MS No. S-2006-331 received August 13, 2006, and reviewed under Institute publication policies. Pertinent discussion including author's closure, if any, will be published in the September-October 2008 *ACI Structural Journal* if the discussion is received by May 1, 2008.

Dionysios A. Bournas *is a PhD Student in the Department of Civil Engineering at the University of Patras, Patras, Greece. His research interests include strengthening of reinforced concrete with advanced composites.*

Panagiota V. Lontou *is a former MSc Student in the Department of Civil Engineering at the University of Patras. Her research interests include strengthening of reinforced concrete with advanced composites.*

Catherine G. Papanicolaou *is a Lecturer in the Department of Civil Engineering at the University of Patras. She received her diploma and PhD from the University of Patras in 1996 and 2003, respectively. Her research interests include high-performance concrete (with emphasis on textile reinforcement) and optimization of advanced prefabrication systems.*

ACI member **Thanasis C. Triantafillou** *is a Professor of civil engineering and Director of the Structural Materials Laboratory at the University of Patras. He received his diploma in civil engineering from the University of Patras in 1985 and his MSc and PhD from the Massachusetts Institute of Technology, Cambridge, MA, in 1987 and 1989, respectively. His research interests include the application of advanced polymer or cement-based composites in combination with concrete, masonry, and timber, with an emphasis on strengthening and seismic retrofitting.*

Certain problems associated with epoxy resins, however, are still to be addressed. A solution of great potential, involving the combination of textiles with cement-based mortars (TRM), has been explored in previous studies on confinement of plain concrete. These materials are experimentally investigated for the first time herein as a means of confining poorly detailed RC columns with limited deformation capacity under seismic loads due to buckling of the longitudinal bars. Comparisons with FRP-retrofitted counterpart specimens allow for the evaluation of the effectiveness of TRM versus FRP jackets.

CONFINEMENT OF REINFORCED CONCRETE IN CONCENTRIC COMPRESSION

Experimental program

The experimental program in this part of the study aimed to compare the effectiveness of TRM versus FRP jackets as a measure of confining RC members. To examine this, 15 short RC prisms were tested under concentric compression. Specimens had a 200 x 200 mm (7.87 x 7.87 in.) cross section representing columns at approximately 2/3 scale. The four corners of all specimens were rounded at a radius equal to 25 mm (0.98 in.). Due to restrictions of the available testing machine as well as for other practical reasons, specimen height was only 380 mm (14.96 in.), implying the possible development of spurious confinement supplied by the platens in the end zones. Because this platen confinement was the same in all specimens tested in pairs to compare TRM versus FRP jackets, which was the main focus of the present investigation, no further consideration was given to the possible effect of end confinement. It is believed that the geometry and detailing chosen in this part of the study sufficiently reproduces the behavior of compression zones in RC members where bar buckling is a scenario limiting deformation capacity.

The prisms were divided in three series, with five specimens each. The first series comprised specimens with no internal steel reinforcement (Series U). The prisms in the second and third series were reinforced with four longitudinal 12 mm (0.47 in.) diameter bars placed at the corners of the cross section at an effective depth equal to 166 mm (6.54 in.) and with 8 mm (0.31 in) diameter stirrups with 135-degree hooks at both ends. Specimen geometry is depicted in Fig. 1. Both longitudinal bars and stirrups were made of deformed steel. Note that the main interest in this study as far as the steel reinforcement is concerned was the spacing of stirrups. Hence, the second series comprised stirrups at a relatively large spacing of 200 mm (7.87 in.) (Series s200) to emulate old detailing practices. In the last series (s100), the spacing was much smaller, equal to 100 mm (3.94 in.), to represent current detailing practices. Other parameters related to the type of steel, bar diameter, and type of hooks were not of interest in this investigation. Each of the three series comprised five different specimens: the control specimen (without wrapping), specimens wrapped with two or three layers of FRP, and specimens wrapped with four or six layers of TRM. Note that the layers in the TRM-jacketed prisms were twice as many compared with their FRP counterparts, resulting in two equivalent confining systems, that is, with equal stiffness and strength in the circumferential direction. (As explained as follows, the fibers of the two jacketing systems in the circumferential direction were of the same type and nearly twice as many in the FRP system compared with the TRM system.) In summary, this experimental program aimed to compare the effectiveness of TRM jackets versus their equivalent FRP jackets on the basis of three parameters: the use of internal steel reinforcement, the spacing of stirrups, and the volumetric ratio of jacketing material (number of layers). All types of specimens are summarized in the first column of Table 1. The notation of specimens is X_YN, where X refers to the internal steel reinforcement (U, s200, s100), Y denotes the type of jacket (C for the unjacketed [control] prisms, R for resin-based jackets, and M for mortar-based jackets), and N denotes the number of layers.

The longitudinal bars had a yield stress of 563 MPa (81.66 ksi), a tensile strength of 658 MPa (95.44 ksi), and an

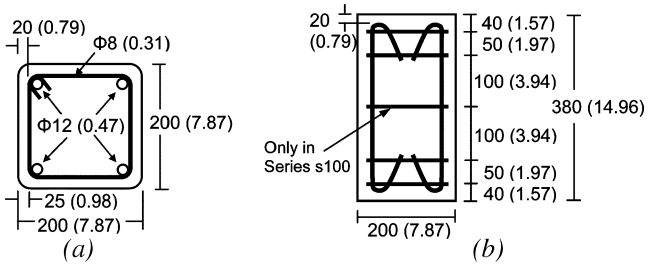

Fig. 1—(a) Cross section of prisms; and (b) configuration of reinforcement. (Dimensions in mm; those in parentheses are in inches.)

Table 1—Strength and deformation capacity of prisms under concentric compression

Specimen notation	Compressive strength		Ultimate strain, %	K_σ	K_ε	$K_\sigma/K_{\sigma,R}$	$K_\varepsilon/K_{\varepsilon,R}$
	MPa	psi					
U_C	15.28	2216	0.29	1.00	1.00	N/A	N/A
U_R2	30.59	4437	0.82	2.00	2.83	1.00	1.00
U_M4	26.60	3858	0.76	1.74	2.62	0.87	0.92
U_R3	34.71	5034	1.28	2.27	4.41	1.00	1.00
U_M6	31.55	4576	1.06	2.06	3.65	0.91	0.83
s200_C	22.89	3320	0.53	1.00	1.00	N/A	N/A
s200_R2	37.27	5406	1.28	1.91	2.41	1.00	1.00
s200_M4	34.24	4966	1.12	1.72	2.16	0.90	0.90
s200_R3	44.65	6476	1.48	2.38	2.79	1.00	1.00
s200_M6	36.03	5226	1.33	1.84	2.50	0.77	0.90
s100_C	24.11	3497	0.69	1.00	1.00	N/A	N/A
s100_R2	41.97	6087	1.32	2.05	1.91	1.00	1.00
s100_M4	38.28	5552	1.26	1.84	1.83	0.90	0.96
s100_R3	45.23	6560	1.72	2.25	2.49	1.00	1.00
s100_M6	39.91	5789	1.50	1.93	2.17	0.86	0.87

ultimate strain equal to 10% (average values from three specimens). Casting of the specimens was made with a single batch of ready mixed concrete in stiff steel molds, with a 28-day strength measured on 150 x150 mm (5.9 x 5.9 in.) cubes equal to 24.65 MPa (3575 psi).

For the specimens receiving TRM jacketing (U_M4, U_M6, s200_M4, s200_M6, s100_M4, and s100_M6), a commercial textile with equal quantity of high-strength carbon rovings in two orthogonal directions was used (Fig. 2(a)). Each fiber roving was 3 mm (0.12 in.) wide and the clear spacing between rovings was 7 mm (0.28 in.). The weight of carbon fibers in the textile was 348 g/m^2 (1.42 × 10^{-6} lb/in.^{2}) and the nominal thickness of each layer (based on the equivalent smeared distribution of fibers) was 0.095 mm (0.0037 in.). The mean tensile strength of the carbon fibers (as well as of the textile when the nominal thickness is used) was taken from data sheets equal to 3800 MPa (551.17 ksi). The elastic modulus of carbon fibers was 225 GPa (32,635 ksi). For the specimens receiving FRP jacketing (U_R2, U_R3, s200_R2, s200_R3, s100_R2, and s100_R3), a commercial unidirectional carbon fiber sheet was used with a weight of 300 g/m^2 (1.22 × 10^{-6} lb/in.^{2}) and a nominal thickness of 0.17 mm (0.0067 in.). The fibers in both the textile and the unidirectional sheet were of the same type. For the specimens receiving mortar as a binding material, a commercial inorganic dry binder was used, consisting of cement and polymers at a ratio of approximately 8:1 by weight. The water:binder ratio in the mortar was 0.23:1 by weight, resulting in plastic consistency and good workability. Finally, for the specimens receiving resin adhesive bonding, a commercial structural adhesive (two-part epoxy resin with a mixing ratio 3:1 by weight) was used with a tensile strength of 70 MPa (10.15 ksi) and an elastic modulus of 3.2 GPa (464 ksi) (cured 7 days at 23 °C [73 °F]). The adhesive had a low viscosity such that complete wetting of the sheets was possible by using a plastic roller.

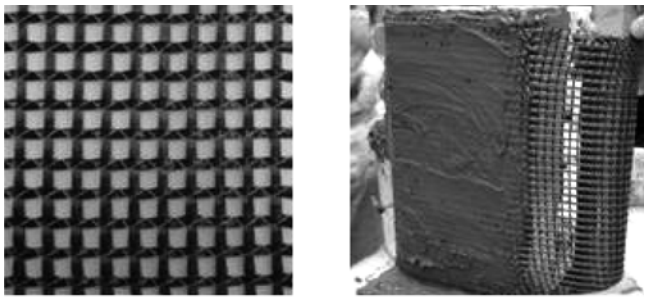

Fig. 2—(a) Photograph of textile used in this study; and (b) application of TRM jacket.

Application of the mortar was made in approximately 2 mm (0.08 in.) thick layers with a smooth metal trowel. After application of the first mortar layer on the (dampened) concrete surface, the textile was applied and pressed slightly into the mortar, which protruded through all the perforations between fiber rovings. The next mortar layer covered the textile completely, and the operation was repeated until all textile layers were applied and covered by the mortar. Of crucial importance in this method, as in the case of epoxy resins, was the application of each mortar layer while the previous one was still in a fresh state. A photograph of the application method of textiles combined with mortar binder to provide jacketing in one of the specimens used in this study is shown in Fig. 2(b).

The strength of mortar used in this study was obtained through flexural and compression testing according to EN 1015-11[24] using a servohydraulic MTS testing machine. Flexural testing was carried out on three 40 x 40 x 160 mm (1.57 x 1.57 x 6.3 in.) hardened mortar prisms at an age of 28 days. The prisms were prepared and cured in the laboratory until testing in conditions identical to those for the jackets used for confinement (except for the first 2 days, when the prisms were inside the molds). The prisms were subjected to three-point bending at a span of 100 mm (3.94 in.), and from the peak load, the flexural strength was calculated. Compression testing was carried out on each of the fractured parts using two 40 x 40 mm (1.57 x 1.57 in.) bearing steel platens on the top and bottom of each specimen. The average flexural and compressive strength values were 6.80 and 22.13 MPa (986 and 3210 psi), respectively.

The response of concrete prisms in concentric compression was obtained through monotonically applied loading at a rate of 0.08 mm/second (0.0031 in./second) in displacement control, using a 4000 kN (900 kip) compression testing machine. Loads were measured by a load cell, and displacements were obtained using external linear variable differential transducers (LVDTs) mounted on two opposite sides at a gauge length of 180 mm (7.09 in.) in the middle part of each specimen. From the applied load, gross section dimensions, and average displacement measurements, the stress-strain curves were obtained for each test.

Test results and discussion

The stress-strain plots recorded for all specimens are given in Fig. 3. Peak stress and ultimate strains are summarized in

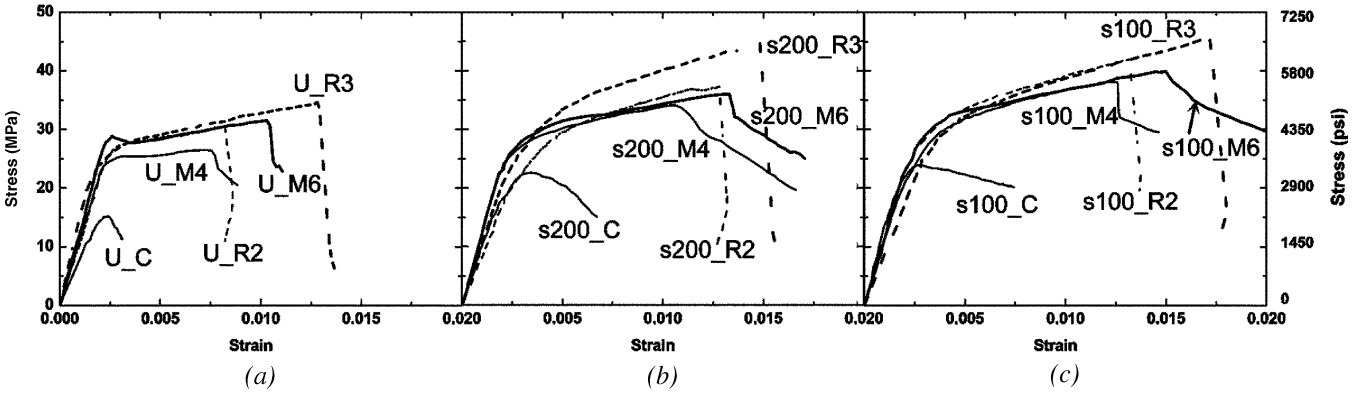

Fig. 3—Stress-strain curves for specimens: (a) without reinforcement; (b) with stirrups at 200 mm (7.87 in.); and (c) with stirrups at 100 mm (3.84 in.).

Table 1. All plots of the confined specimens are characterized by an ascending branch followed by a second one, close to linear, that drops at a point where the jacket fractured due to hoop stresses (Fig. 4(a)). It is this point where peak stress and ultimate strain is defined, except for the control (unjacketed) specimens, where ultimate strain is defined conventionally at 15% peak stress reduction.

In some of the TRM-jacketed prisms (s200_M4 and s100_M6), fracture of the fibers was accompanied by debonding at the end of the lap (Fig. 4(b)). On several occasions, jacket rupture occurred simultaneously with bar buckling. Hence, failure of the jackets was due to stretching both by concrete dilation and by the outward bending of the longitudinal bars in the middle of the specimens (Fig. 4(c)). Similar observations have been made by other researchers as well (refer to, for example, Reference 25). Another important aspect of the response is that, contrary to FRP jackets, TRM jackets did not fail abruptly. As also reported in Reference 1, in the case of TRM jackets, fracture initiates from a limited number of fiber bundles (when the hoop stresses reach their tensile capacity) and then propagates rather slowly in the neighboring bundles, resulting in a more ductile failure mechanism compared with FRP. It is believed that this phenomenon is observed for TRM and not for FRP due to the facts that: a) fiber bundles in TRM jackets are usually not well impregnated and loading of the fibers is done with a nonuniform distribution of forces, possibly leading to telescopic failure (the term telescopic is used herein to describe the relative slip between fibers in the outer part of each roving and those in the core); and b) multiple cracking in the matrix of TRM at low tensile (hoop) stress levels leads to pullout failure at higher stress levels rather than fracture failure of the fibers.

In this study, the jacket confining effectiveness in terms of strength, K_σ, is calculated as the ratio of the peak stress sustained by the encased concrete section of each specimen divided by the concrete-only axial strength of the corresponding control specimen

$$K_\sigma = \frac{\sigma_{max,c} - \frac{A_s}{A_g} f_y}{\sigma_{max,o} - \frac{A_s}{A_g} f_y} \quad (1)$$

where $\sigma_{max,c}$ is the peak stress of confined specimens; $\sigma_{max,o}$ is the peak stress of unconfined specimens; A_g is the gross area of the specimen's cross section; and A_s and f_y are the area and yield strength of longitudinal reinforcement, respectively. Values of K_σ are listed in Table 1, which also gives the jacketing effectiveness in terms of ultimate strain, K_ε, defined as the ratio of the ultimate strain in the confined specimen to that in the corresponding control (unconfined).

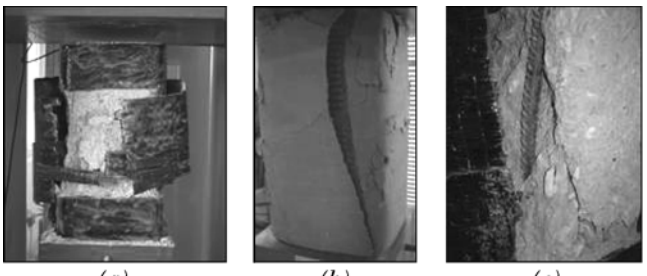

Fig. 4—(a) Fracture of jacket; (b) debonding at end of lap; and (c) buckling of bar at corner.

By comparing the response of specimens with jackets with that of unjacketed specimens, it is concluded that both FRP and, to a slightly lesser degree, TRM confinement, is quite effective in increasing the strength and deformation capacity of concentrically loaded prisms as well as in delaying buckling of longitudinal bars. The average effectiveness in terms of strength (K_σ) was approximately 2 (average of 2.0, 1.91, and 2.05 in Table 1) for two-layered FRP jackets and approximately 2.3 for three-layered FRP jackets. In the case of TRM jackets, the corresponding values were 1.77 and 1.94. A comparison of the effectiveness of mortar-based (TRM) versus resin-based (FRP) jackets can be made by dividing the values of K_σ for TRM with their FRP counterparts ($K_\sigma/K_{\sigma,R}$ in Table 1). This ratio is approximately 0.9 for the lower number of layers (two FRP or four TRM) and approximately 0.85 for the higher number of layers (three FRP or six TRM).

Similar comparisons can be made in terms of ultimate strain defined at conventional failure. Herein, the jacket effectiveness K_ε increased with the number of layers but decreased with the increase in confinement provided by stirrups. K_ε was in the range 2.83 to 1.91 for two-layered FRP jackets and 4.41 to 2.49 for three-layered FRP jackets. In the case of TRM jackets, the corresponding values were lower, on average by 7% for four layers (equivalent to two FRP) and by 13% for six layers (equivalent to three FRP). The effectiveness of mortar-based (TRM) versus resin-based (FRP) jackets in terms of strain at conventional failure can be made by dividing the corresponding K_ε values ($K_\varepsilon/K_{\varepsilon,R}$ in Table 1). This ratio is approximately 0.93 for the lower number of layers (two FRP or four TRM) and approximately 0.87 for the higher number of layers (three FRP or six TRM).

The quantitative conclusions given previously should be taken with care, as they are based on rather limited testing with specific materials. Other materials (for example, different mortars) may result in different values for the effectiveness of TRM versus FRP as a function of the number of layers. Overall, it may be concluded that TRM confining jackets provide substantial gain in compressive strength and deformation capacity of concentrically loaded RC prisms by delaying buckling of the longitudinal reinforcing bars. Compared with equal stiffness and strength, FRP jackets are characterized by a slightly reduced effectiveness. On the basis of the results presented in this study, this reduction seems to be independent of the volumetric ratio of embedded stirrup reinforcement. A possible reason for the reduced effectiveness of TRM versus FRP is that, in the TRM system, the distribution of stresses in the fibers is much more nonuniform in comparison with the FRP system due to slippage and local debonding (between fibers as well as between fibers and the matrix) and due to microcracking of the matrix (mortar).

LOCAL CONFINEMENT OF OLD-TYPE REINFORCED CONCRETE COLUMNS

Experimental program

The experimental program in this part of the study aimed to compare the effectiveness of TRM versus FRP jackets applied at the ends of old-type RC columns as a measure of improving the deformation capacity during simulated seismic loading. Three full-scale RC column specimens with the same geometry and reinforcement were constructed and tested under lateral load (Fig. 5). The specimens were flexure-

dominated cantilevers with a height to the point of application of the load (shear span) of 1.6 m (63 in.) (half a typical story height) and a cross section of 250 x 250 mm (9.84 x 9.84 in.).

One specimen was tested without retrofitting as a control (C), the second one was retrofitted with two layers of a CFRP jacket (Specimen R2), and the third one was retrofitted with an equal (to its FRP counterpart) stiffness and strength TRM jacket comprising four layers (Specimen M4). Specimen notation is such as to define the type of binder used (resin or mortar) and the number of layers. The jackets extended from the base of each column (a gap of approximately 10 mm [0.39 in.] was left) to a height of 430 mm (16.93 in.). Before jacketing, the four corners of the two columns that received jacketing were rounded at a radius equal to 25 mm (0.98 in.).

The columns were fixed into a heavily reinforced 0.5 m (19.68 in.) deep base block, 1.2 x 0.5 m (47 x 19.7 in.) in plan, within which the longitudinal bars were anchored with 70 mm (2.76 in.) radius hooks at the bottom. To represent old-type nonseismically designed and detailed columns, specimens were reinforced longitudinally with four 14 mm (0.55 in.) diameter smooth bars with an effective depth of 215 mm (8.46 in.) and 8 mm (0.31 in.) diameter smooth stirrups at a spacing of 200 mm (7.87 in.). The stirrups were closed with 90-degree hooks at both ends.

The longitudinal bars had a yield stress of 372 MPa (54 ksi), a tensile strength of 433 MPa (62.8 ksi), and an ultimate strain equal to 17% (average values from three specimens). The corresponding values for the steel used for stirrups were 351 MPa (50.9 ksi), 444 MPa (64.4 ksi), and 19.5%. Casting of the specimens was made with a single batch of ready mixed concrete, with a 28-day strength measured on 150 x 150 mm (5.9 x 5.9 in.) cubes equal to 25 MPa (3625 psi). The TRM and FRP materials used to retrofit Specimens M4 and R2, respectively, were the same as those described in the previous section; likewise for the method of application.

The columns were subjected to lateral cyclic loading (successive cycles progressively increasing by 5 mm [0.2 in.] of displacement amplitudes in each direction at a rate ranging from 0.2 to 1.1 mm/second [0.008 to 0.043 in./second], the higher rate corresponding to a higher displacement amplitude, all in displacement-control mode) under a constant axial compressive load of 460 kN (103 kips) corresponding to 30% of the member's compressive strength. The lateral load was applied using a horizontally positioned 250 kN (56 kips) MTS actuator and the axial load was exerted by a set of four hydraulic cylinders acting against two vertical rods connected to the strong floor of the testing frame through a hinge (Fig. 5(b) and 6(a)). With this setup, the P-Δ moment at the base section of the column was equal to the axial load times the tip deflection (that is, at piston fixing position) of the column, times the ratio of hinge distance from the base (0.25 m) and the top (0.25 + 1.60 = 1.85 m) of the column (that is, times 0.25/1.85 = 0.135).

Displacements at the plastic hinge region were monitored using six rectilinear displacement transducers (three on each side perpendicular to the piston axis) fixed at Cross Sections 1, 2, and 3 with a distance equal to l_1 = 130 mm (5.12 in.), l_2 = 260 mm (10.24 in.), and l_3 = 450 mm (17.72 in.), respectively, from the column base, as shown in Fig. 6(b).

Test results and discussion

Test results are presented in Fig. 7 in the form of load-displacement (horizontal deflection at the point of load application) loops. Key results are also presented in Table 2; they include: a) the peak resistance in the two directions of loading; b) the drift ratio (obtained by dividing the tip deflection with the specimens' height) corresponding to peak resistance in the two directions of loading; c) the drift ratio at conventional failure of the column, defined as a reduction of peak resistance in a cycle below 85% of the maximum recorded resistance in that direction of loading; and d) the curvature at failure of the column, conventionally defined as in (c)—that curvature takes place at the same time and in the same direction as failure defined on the basis of drift. The curvature was derived from the relative rotation measured over the lower 130 mm (5.1 in.) of the column above the base, including the column section at the face of the footing and the effect of bar pullout from the base. More specifically, the curvature was calculated by dividing the rotation θ_1 of the cross section at l_1 = 130 mm (5.1 in.) (calculated by dividing the sum of displacements recorded by the two transducers at opposite sides with their horizontal distance) with the distance of this section from the column base (130 mm [5.1 in.]).

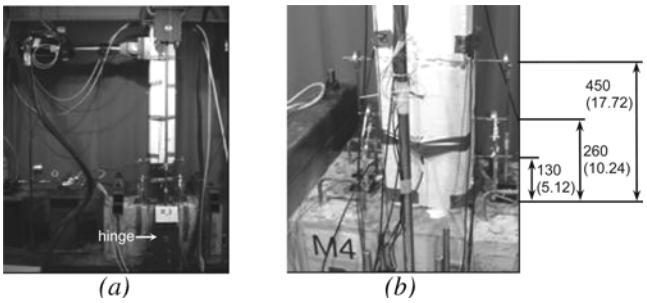

Fig. 6—(a) Photograph of test setup; and (b) position of displacement transducers. (Dimensions in mm, those in parentheses are in inches.)

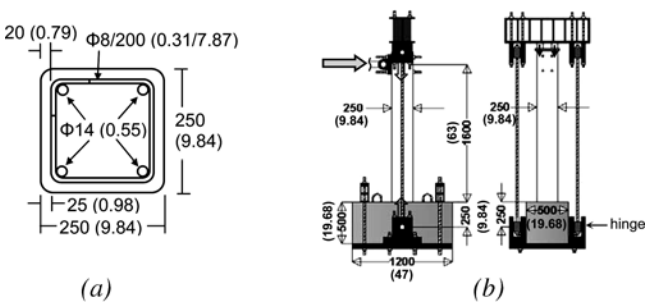

Fig. 5—(a) Cross section of columns; and (b) schematic of test setup. (Dimensions in mm; those in parentheses are in inches.)

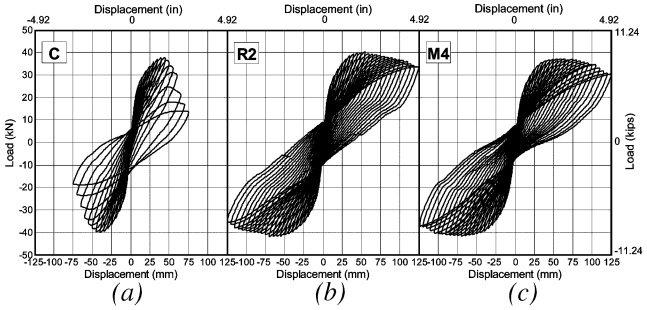

Fig. 7—Load-displacement curves for: (a) unretrofitted column (C); (b) FRP-retrofitted column (R2); and (c) TRM-retrofitted column (M4).

The performance and failure mode of all tested columns was controlled by flexure. The unretrofitted column (Fig. 7(a)) attained a drift ratio at failure of approximately 3.75%. The concrete cover and part of the core over the lower 200 mm (7.87 in.) of the column disintegrated and bar buckling initiated after the concrete cover spalled off at a drift ratio of approximately 3% (Fig. 8(a)). The behavior of the two retrofitted columns was very similar (Fig. 7(b) and (c) for Columns R2 and M4, respectively), but quite different from and far better than their unretrofitted counterpart. Member deformation capacity increased by a factor of more than 2, corresponding to a drift ratio at failure of approximately 7.5%; peak resistance was practically the same as in the unretrofitted column, and the post peak response was quite stable, displaying a very gradual strength degradation. Whereas the FRP jacket in Column R2 exhibited limited rupture over the lower 50 mm (1.97 in.) (Fig. 8(b)) at 7.2% drift ratio (in the pull direction), the TRM jacket remained intact until the test was terminated at 7.8% drift ratio (Fig. 8(c)). When the jackets were removed in both retrofitted columns after the end of the tests, a completely disintegrated concrete core was exposed, one that had been kept in place by the heavy confinement provided by the jackets (both FRP and TRM).

Figure 9 shows the evolution during the test of the mean axial strain at the opposite sides of the column within the bottom 260 mm (10.24 in.) of its height, as derived from the individual displacement transducer measurements. Negative strains reflect compressive deformation of the concrete in the lower 260 mm (10.24 in.) of the column and, near the end of the unretrofitted column test, bar buckling. In the two retrofitted columns, the large magnitude of measured compressive strains (close to 6%) demonstrates the very large effect of confinement by the jackets. Positive strains include the effect of crack opening and bar pullout, smeared over the gauge length of 260 mm (10.24 in.). The small magnitude of the difference (in the order of 10%) between the positive displacements measured over the bottom 130 mm (5.12 in.) from those measured over the bottom 260 mm (10.24 in.) suggests that the major part of these displacements (and, hence, of the positive strains in Fig. 9) is due to substantial crack opening at the base and bar pullout, especially in the retrofitted columns. The large crack opening at the base of the columns is confirmed by the plots shown in Fig. 10, which provide the relationship between crack width at the base and drift ratio. The crack width was calculated as $w = \Delta l_2 - \varepsilon_{flex} l_2 = \Delta l_1 - \varepsilon_{flex} l_1$, where Δl_1 and Δl_2 are the elongations measured by the displacement transducers at Cross Sections 1 and 2, respectively, and ε_{flex} is the mean strain in the extreme tension fiber at the column base, equal to $(\Delta l_2 - \Delta l_1)/(l_2 - l_1)$. This crack width-drift ratio relationship is approximately linear and, in the two retrofitted columns, nearly the same. The maximum values of crack opening at conventional failure were approximately 5, 15, and 15 mm (0.2, 0.59, and 0.59 in.) for Specimens C, R2, and M4, respectively.

Figure 11 gives the relation between the drift ratio and the slip rotation θ_{slip} of the cross section at the interface between the column and the base. The latter was measured using the data from displacement transducers in two cross sections at distance l_1 = 130 mm (5.12 in.) and l_2 = 260 mm (10.24 in.) from the base as follows: $\theta_{slip} = \theta_2 - \phi l_2 = \theta_1 - \phi l_1$ where ϕ is the mean curvature at the column base, equal to $(\theta_2 - \theta_1)/(l_2 - l_1)$. In this way, it is possible to estimate the contribution of the slip rotation to the overall column deformation. Two main aspects can be observed: 1) the θ_{slip}-drift ratio relation is nearly linear, especially in the retrofitted columns; and 2) the contribution of slip rotation is prevalent, approximately 70 and 90% of the global drift at failure for the unretrofitted and retrofitted columns, respectively.

In the unretrofitted column, the gradual loss of lateral load resistance during the cycle that led to failure was accompanied

Table 2—Summary of column test results

Specimen notation	Peak force, kN (kip)		Drift at peak force, %		Drift at failure, %		Curvature at failure, mrad/m (mrad/in.)	
	Push	Pull	Push	Pull	Push	Pull	Push	Pull
C	37.92 (8.53)	39.79 (8.95)	2.8	2.8	3.75	3.75	175 (4.45)	164 (4.17)
R2	37.23 (8.37)	41.63 (9.36)	3.4	4.4	7.5	7.5	440 (11.18)	430 (10.92)
M4	40.16 (9.03)	41.75 (9.39)	4.1	4.4	7.5	7.81	420 (10.67)	502 (12.75)

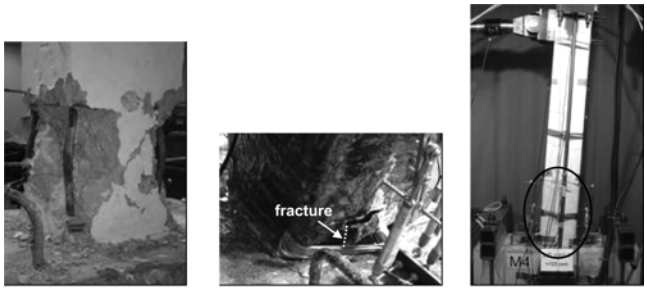

Fig. 8—(a) Disintegration of concrete and bar buckling; (b) limited rupture of FRP jacket; and (c) undamaged TRM jacket at end of test.

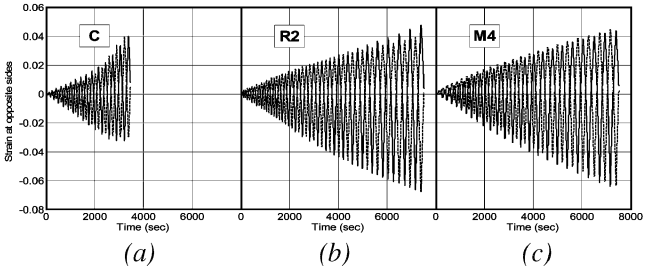

Fig. 9—Evolution of vertical strain at opposite sides of column (mean value over lower 260 mm [10.24 in.] from base): (a) unretrofitted column; (b) FRP retrofitted; and (c) TRM retrofitted.

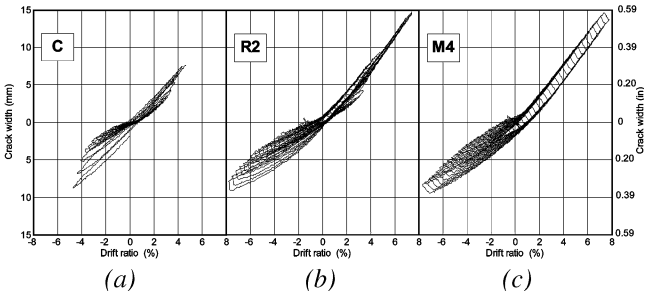

Fig. 10—Measured crack width at base in terms of drift ratio: (a) unretrofitted column; (b) FRP retrofitted; and (c) TRM retrofitted.

by some loss of axial load resistance, evidenced by the difficulty to maintain the axial load constant. Retrofitted columns maintained constant axial load (and practically lateral force) capacity up to the end of the tests.

The evolution of the mean axial strain at the center of the cross section over the bottom 260 mm (10.24 in.) above the base (as derived from the average of the displacement transducer measurements on opposite sides of the column) is an indication of those phenomena within the plastic hinge region that affect axial load resistance. This evolution is shown in Fig. 12 as a function of tip deflection. The change of column length almost in proportion to lateral deflection can be explained as being a direct consequence of flexure according to the plane-sections hypothesis. If less than half of the cross section is in compression, the less deep the compression zone, the larger the column elongation in each deflection cycle. This is confirmed by the present results, which show larger mean elongation per half-cycle with respect to the neutral position (zero deflection) in the retrofitted specimens than in the unretrofitted one. As evidenced in Fig. 12(a), in the unretrofitted column that failed

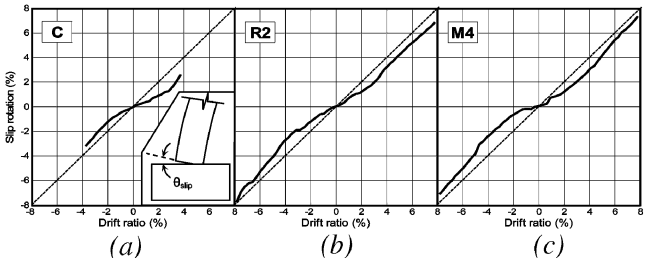

Fig. 11—Slip rotation at base in terms of drift ratio: (a) unretrofitted column; (b) FRP-retrofitted; and (c) TRM retrofitted.

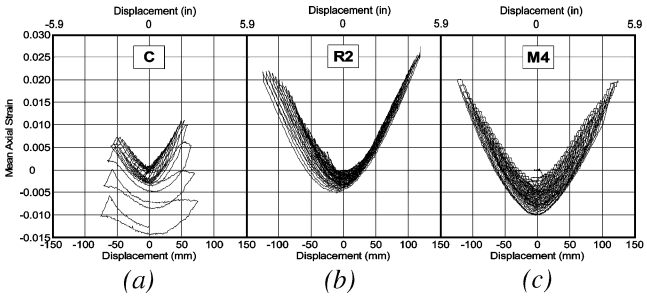

Fig. 12—Evolution of mean vertical strain at center of cross section (over bottom 200 mm [10.24 in.) above base) with tip deflection: (a) unretrofitted column; and (b) FRP retrofitted; and (c) TRM retrofitted.

gradually with bar buckling on both sides and concrete crushing all over the section, mean compressive strains above 1% developed over the bottom 260 mm (10.24 in) of the column around failure. These strains are associated with the difficulty to maintain the axial load constant at that stage. Confinement by jacketing limited the magnitude of these strains; the strain reduction was lower in the case of TRM jacketing (Fig. 12(c)) compared with its FRP counterpart (Fig. 12(b)).

By comparison of the cumulative dissipated energies given in Fig. 13(a) (computed by summing up the area enclosed within the load versus piston displacement curves), it is observed that the energy dissipation capacity of the two retrofitting schemes (TRM versus FRP) is approximately the same. At conventional failure, the energy dissipated by the retrofitted columns was approximately six times higher than that dissipated by the unretrofitted column. Finally, the comparison of the stiffness versus drift ratio shown in Fig. 13(b) illustrates that the stiffness reduction beyond peak load was similar in both retrofitted columns and considerably lower in comparison to the unretrofitted specimen. The last comparison is made with regard to the distribution of curvature at failure along the column height. The plots given in Fig. 13(c) have been produced on the basis of measurements at three cross sections (130, 260, and 450 mm [5.12, 10.24, and 17.72 in.]); they demonstrate that both retrofitted columns have nearly identical curvatures at failure, which exceeded that of the unretrofitted column by a factor of approximately 2.5.

Overall, comparing the behavior of Columns R2 and M4, it is concluded that the force and cyclic deformation capacity, the rate of strength and stiffness degradation, and the energy dissipation of the column jacketed with TRM is practically identical to its FRP counterpart.

Comparison of test results with code formulations

In this section, one important response parameter of the column test results is compared (namely, the drift ratio at failure) with predictions given by Eurocode 8.[26] This quantity, defined as chord rotation capacity at ultimate in Eurocode 8, is given by the following empirical expression

$$\theta_u = k0.016(0.3^{\nu})\left[\frac{\max(0.01, \omega')}{\max(0.01, \omega)} f_c\right]^{0.225}\left(\frac{L_V}{h}\right)^{0.35} \cdot \qquad (2)$$

$$25^{c}(1.25^{100\rho_d})$$

where f_c is the compressive strength of concrete (MPa); ω and ω' are the mechanical reinforcement ratio of tension and compression longitudinal reinforcement, respectively; $\nu = N/bhf_c$ is the normalized axial force (compression taken as

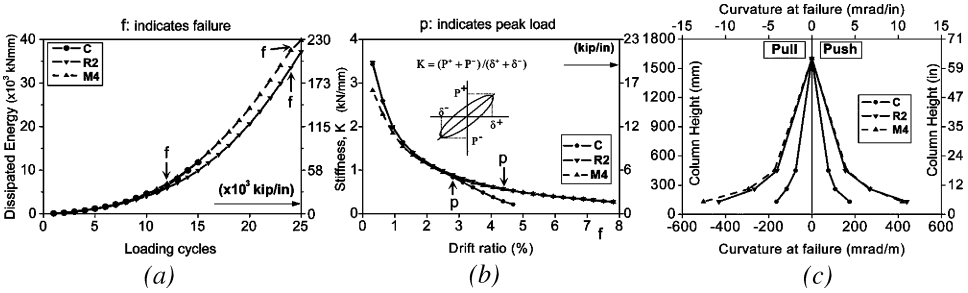

Fig. 13—(a) Cumulative dissipated energy during test; (b) stiffness versus drift ratio; and (c) curvature at failure along column height.

positive where b is the width of compression zone and h is the cross section side parallel to the loading direction); $L_V = M/V$ is the ratio of moment/shear at the end section; $c = \alpha\rho_{sx}f_{yw}/f_c$; $\rho_{sx} = A_{sw}/bs_h$ is the transverse steel ratio parallel to the direction x of loading; f_{yw} is the yield stress of stirrups; $k = 0.575$ for columns with smooth bars; ρ_d is the geometric ratio of diagonal reinforcement, if any; and α is the effectiveness coefficient for confinement with stirrups.

If a column is retrofitted with an FRP or TRM jacket in the plastic hinge region, it is logical to adopt the expression in Eq. (2) with c given by the sum of two terms: one to account for the contribution of stirrups and a second one to account for the contribution of the jacket, as follows

$$c = a\rho_{sx}\frac{f_{yw}}{f_c} + a_f\rho_{fx}\frac{f_{fe}}{f_c} \quad (3)$$

where $\rho_{fx} = 2nt_f/b$; n is the number of layers of the fiber sheet or textile; t_f is the thickness of one fiber sheet or textile layer; f_{fe} is the effective strength of jacket; and α_f is the effectiveness coefficient for confinement with fibers (TRM or FRP jackets), equal to

$$\alpha_f = \beta\left[1 - \frac{(b-2R)^2 + (h-2R)^2}{3bh}\right] \quad (4)$$

where R is the radius at the corners of the cross section. The coefficient β in Eq. (4) is proposed herein to account for the reduced effectiveness of TRM versus FRP jackets in terms of ultimate strain (on the basis of the concentric compression prism tests presented in the previous section, this value, equal to $K_\varepsilon/K_{\varepsilon,R}$ in Table 1, is approximately 0.9). But if jacket failure has not been reached at conventional failure of the column, no reduction should be made and β should be taken equal to 1.

For the geometric and material properties of the columns tested in this study, the values calculated for θ_u are 2.60%, 4.30%, and 4.46% for Columns, C, R2 and M4, respectively. The corresponding experimental values (mean values in the push and pull directions; refer to Table 2) are 3.75%, 7.50%, and 7.65%. Hence, the predicted drift ratios at failure according to Eurocode 8-based approach described previously, are 31% and 42 to 43% lower than the experimental values for the unretrofitted and retrofitted columns, respectively. This fact leads to the conclusion that, when compared with the test results presented in this study, the Eurocode 8-based formulation presented previously (for columns with smooth bars) is conservative, especially for members jacketed with FRP or TRM.

CONCLUSIONS

The effectiveness of TRM jackets as a means of confining RC columns with limited capacity due to buckling of the longitudinal bars is investigated in this study. Comparisons with FRP jackets of equal stiffness and strength allow for the evaluation of the effectiveness of TRM versus FRP jackets.

The 15 concentric compression tests performed in this study on RC prisms show that TRM confining jackets provide substantial gain in compressive strength and deformation capacity by delaying buckling of the longitudinal bars; this gain increases with the volumetric ratio of the TRM wrap. Compared with FRP jackets of equal stiffness and strength, the TRM jackets used in this study are slightly less effective in terms of increasing strength and deformation capacity by approximately 10%. On the basis of the rather limited test results presented herein, it seems that this reduction in effectiveness does not depend on the volumetric ratio of embedded stirrup reinforcement.

The three tests on nearly full-scale columns under cyclic uniaxial flexure show that TRM jackets are very effective as a means of increasing the cyclic deformation capacity and the energy dissipation of old-type RC columns with poor detailing, by delaying bar buckling. Compared with equal stiffness and strength FRP, TRM jacketing has practically the same effectiveness.

Despite their relatively limited number, all test results presented in this study indicate that TRM jacketing is an extremely promising solution for the confinement of RC columns, including poorly detailed ones in seismic regions.

ACKNOWLEDGMENTS

The authors wish to thank S. Bousias, K. Zygouris, N. Caicedo, F. Stavropoulos, A. Reisi, and C. Petropoulos for their assistance in the experimental program. The work reported in this paper was funded by the Greek General Secretariat for Research and Technology, through the project ARISTION, within the framework of the program Built Environment and Management of Seismic Risk.

NOTATION

A_g	=	gross section area
A_s	=	area of longitudinal reinforcement
A_{sw}	=	area of transverse steel reinforcement parallel to direction x within s_h
b	=	cross section width, width of compression zone
f_c	=	compressive strength of concrete
f_{fe}	=	effective tensile strength of jacket
f_y	=	yield strength of longitudinal reinforcement
f_{yw}	=	yield stress of stirrups
h	=	cross section height, side parallel to loading direction
K	=	stiffness
K_ε	=	jacket confining effectiveness in terms of strain
$K_{\varepsilon,R}$	=	resin-based jacket confining effectiveness in terms of strain
K_σ	=	jacket confining effectiveness in terms of strength
$K_{\sigma,R}$	=	resin-based jacket confining effectiveness in terms of strength
k	=	coefficient
L_V	=	ratio of moment/shear at end section
l_i	=	distance of cross section i from column base, $i = 1, 2, 3$
M	=	moment at end section
N	=	axial force
n	=	number of layers
R	=	radius at corners of cross section
s_h	=	spacing of stirrups
t_f	=	thickness of one fiber sheet or textile layer
V	=	shear at end section
w	=	crack width
x	=	direction of loading
α	=	effectiveness coefficient for confinement with stirrups
α_f	=	effectiveness coefficient for confinement with fibers
β	=	TRM versus FRP jacket confining effectiveness in terms of strength
Δl_i	=	elongation of displacement transducer at section i, $i = 1, 2$
ε_{flex}	=	mean strain in the extreme tension fiber at column base
ϕ	=	mean curvature at column base
ν	=	normalized axial force
θ_i	=	rotation of cross section i, $i = 1, 2$
θ_{slip}	=	slip rotation at column base
θ_u	=	chord rotation at ultimate
ρ_d	=	geometric ratio of diagonal reinforcement
ρ_{fx}	=	ratio of fibers parallel to direction x of loading
ρ_{sx}	=	transverse steel ratio parallel to direction x of loading
$\sigma_{max,c}$	=	peak stress of confined specimens
$\sigma_{max,o}$	=	peak stress of unconfined specimens
ω	=	mechanical reinforcement ratio of tension longitudinal reinforcement
ω'	=	mechanical reinforcement ratio of compression longitudinal reinforcement

REFERENCES

1. Triantafillou, T. C.; Papanicolaou, C. G.; Zissimopoulos, P.; and Laourdekis, T., "Concrete Confinement with Textile-Reinforced Mortar Jackets," *ACI Structural Journal*, V. 103, No. 1, Jan.-Feb. 2006, pp. 28-37.

2. Bischoff, T.; Wulfhorst, B.; Franzke, G.; Offermann, P.; Bartl, A.-M.; Fuchs, H.; Hempel, R.; Curbach, M.; Pachow, U.; and Weiser, W., "Textile Reinforced Concrete Façade Elements—An Investigation to Optimize Concrete Composite Technologies," *43rd International SAMPE Symposium*, 1998, pp. 1790-1802.

3. Curbach, M., and Jesse, F., "High-Performance Textile-Reinforced Concrete," *Structural Engineering International*, IABSE, V. 4, 1999, pp. 289-291.

4. Sato, Y.; Fujii, S.; Seto, Y.; and Fujii, T., "Structural Behavior of Composite Reinforced Concrete Members Encased by Continuous Fiber-Mesh Reinforced Mortar Permanent Forms," *Fiber Reinforced Polymer Reinforcement for Reinforced Concrete Structures*, SP-188, C. W. Dolan, S. H. Rizkalla, and A. Nanni, eds., American Concrete Institute, Farmington Hills, MI, 1999, pp. 113-124.

5. Brameshuber, W.; Brockmann, J.; and Roessler, G., "Textile Reinforced Concrete for Formwork Elements—Investigations of Structural Behaviour," *FRPRCS-5 Fiber Reinforced Plastics for Reinforced Concrete Structures*, V. 2, C. J. Burgoyne, ed., Thomas Telford, London, UK, 2001, pp. 1019-1026.

6. Molter, M.; Littwin, R.; and Hegger, J., "Cracking and Failure Modes of Textile Reinforced Concrete," *FRPRCS-5 Fiber Reinforced Plastics for Reinforced Concrete Structures*, V. 2, C. J. Burgoyne, ed., Thomas Telford, London, UK, 2001, pp. 1009-1018.

7. Mu, B., and Meyer, C., "Flexural Behavior of Fiber Mesh-Reinforced Concrete with Glass Aggregate," *ACI Materials Journal*, V. 99, No. 5, Sept.-Oct. 2002, pp. 425-434.

8. Nakai, H.; Terada, N.; Honma, A.; and Nishikawa, K., "Improvement in Performance of Concrete Structures by Using Sandy Fiber Mesh," *1st fib Congress*, Session 8, Osaka, Japan, 2002, pp. 325-332.

9. Naaman, A. E., "Progress in Ferrocement and Textile Hybrid Composites," *2nd Colloquium on Textile Reinforced Structures*, M. Curbach, ed., Dresden, 2003, pp. 325-346.

10. Reinhardt, H. W.; Krueger, M.; and Grosse, C. U., "Concrete Prestressed with Textile Fabric," *Journal of Advanced Concrete Technology*, V. 1, No. 3, 2003, pp. 231-239.

11. Banholzer, B., and Brameshuber, W., "Lost Formwork Elements made of Textile Reinforced Concrete," *fib Symposium Keep Concrete Attractive*, Budapest, Hungary, 2005, pp. 351-356.

12. Brockmann, T., and Brameshuber, W., "Matrix Development for the Production Technology of Textile Reinforced Concrete (TRC) Structural Elements," *3rd International Conference on Composites in Construction,* Lyon, France, 2005, pp. 1165-1172.

13. Inoue, M.; Takagi, N.; and Kojima, T., "Behaviour of RC Beams using Highly Durable Permanent Formwork made of Three-Dimensional Hollow Structure Glass Fabric," *ConMat'05 and Mindess Symposium—Construction Materials*, N. Banthia, T. Uomoto, A. Bentur, and S. P. Shah, eds., The University of British Columbia, BC, Canada, 2005.

14. Peled, A., and Mobasher, B., "Pultruded Fabric-Cement Composites," *ACI Materials Journal*, V. 102, No. 1, Jan.-Feb. 2005, pp. 15-23.

15. Roye, A., and Gries, T., "Tensile Behavior of Rovings, Textiles and Concrete Elements—Possible to Compare Directly?" *3rd International Conference on Composites in Construction*, Lyon, France, 2005, pp. 1147-1154.

16. Hegger, J., and Voss, S., "Design Methods for Textile Reinforced Concrete under Bending and Shear Loading," *2nd International fib Congress*, Session 14, Naples, Italy, 2006.

17. Hegger, J., and Niewels, J., "Processing of a Carbon Textile as Concrete Reinforcement," *2nd International fib Congress*, Session 14, Naples, Italy, 2006.

18. Curbach, M., and Ortlepp, R., "Besonderheiten des Verbundverhaltens von Verstaerkungsschichten aus textilbewehrtem," *2nd Colloquium on Textile Reinforced Structures*, M. Curbach, ed., Dresden, 2003, pp. 361-374. (in German)

19. Curbach, M., and Brueckner, A., "Textile Strukturen zur Querkraftverstaerkung von Stahlbetonbauteilen," *2nd Colloquium on Textile Reinforced Structures*, M. Curbach, ed., Dresden, 2003, pp. 347-360. (in German)

20. Brueckner, A.; Ortlepp, R.; Weiland, S.; and Curbach, M., "Shear Strengthening with Textile Reinforced Concrete," *3rd International Conference on Composites in Construction*, Lyon, France, 2005, pp. 1307-1314.

21. Weiland, S.; Ortlepp, R.; and Curbach, M., "Strengthening of Predeformed Slabs with Textile Reinforced Concrete," *2nd International fib Congress*, Session 14, Naples, Italy, 2006.

22. Triantafillou, T. C., and Papanicolaou, C. G., "Shear Strengthening of Reinforced Concrete Members with Textile Reinforced Mortar (TRM) Jackets," *RILEM Materials and Structures*, V. 39, No. 1, 2006, pp. 85-93.

23. Triantafillou, T. C., and Papanicolaou, C. G., "Textile Reinforced Mortars (TRM) versus Fiber Reinforced Polymers (FRP) for Concrete Confinement," *ConMat'05 and Mindess Symposium—Construction Materials*, N. Banthia, T. Uomoto, A. Bentur, and S. P. Shah, eds., University of British Columbia, BC, Canada, 2005.

24. EN 1015-11, *Methods of Test for Mortar for Masonry—Part 11: Determination of Flexural and Compressive Strength of Hardened Mortar*, European Committee for Standardization, Brussels, Belgium, 1993.

25. Tastani, S. P.; Pantazopoulou, S. J.; Zdoumba, D.; Plakantaras, V.; and Akritidis, E., "Limitations of FRP Jacketing in Confining Old-Type Reinforced Concrete Members in Axial Compression," *Journal of Composites for Construction*, ASCE, V. 10, No. 1, 2006, pp. 13-25.

26. EN 1998-3, "Eurocode 8: Design of Structures for Earthquake Resistance—Part 3: Assessment and Retrofitting of Buildings," European Committee for Standardization, Brussels, Belgium, 2005.